A Physically-Informed, Circuit-Bendable, Digital Model of the Roland TR-808 Bass Drum Circuit

3 authors, including:

Kurt James Werner
Queen's University Belfast
35 PUBLICATIONS   152 CITATIONS

Julius Smith
Stanford University
347 PUBLICATIONS   6,746 CITATIONS

Some of the authors of this publication are also working on these related projects:

Physical model of a drum: FDTD techniques combined with a room acoustics model   View project

Create new project "Acoustical Society Presentations"   View project

A PHYSICALLY-INFORMED, CIRCUIT-BENDABLE, DIGITAL MODEL OF THE ROLAND TR-808 BASS DRUM CIRCUIT

Kurt James Werner, Jonathan S. Abel, Julius O. Smith III,

Center for Computer Research in Music and Acoustics (CCRMA)
Stanford University, Stanford, California
`[kwerner|abel|jos]@ccrma.stanford.edu`

ABSTRACT

We present an analysis of the bass drum circuit from the classic Roland TR-808 Rhythm Composer, based on physical models of the device's many sub-circuits. A digital model based on this analysis (implemented in Cycling 74's `Gen~`) retains the salient features of the original and allows accurate emulation of circuit-bent modifications—complicated behavior that is impossible to capture through black-box modeling or structured sampling. Additionally, this analysis will clear up common misconceptions about the circuit, support the design of further drum machine modifications, and form a foundation for circuit-based musicological inquiry into the history of analog drum machines.

1. INTRODUCTION

When Roland discontinued the TR-808 Rhythm Composer in 1984, it was considered somewhat of a flop—despite significant voice design innovations, disappointing sales and a lukewarm critical reception seemed clear indicators that digitally-sampled drum machines were the future. Ironically, this lack of interest drove second-hand prices down and made it an attractive source of beats for techno and hip-hop producers. It soon became ubiquitous, playing a central role in the development of acid house. More than a decade later, when the Beastie Boys rapped "nothing sounds quite like an 808" [2], no one disagreed.

To this day, the 808 remains a benchmark against which all other analog drum machines are measured. Among all of its voices, perhaps the most influential has been the bass drum, the thumping foundation of countless four-on-the-floor dance beats. It could be tweaked via stock user controls to sound like a fairly realistic kick, or extended beyond recognition to a multi-second-long decaying pseudo-sinusoid with a characteristic sighing pitch. Its clicky attack could cut through a mix, but could be dialed back with a passive tone control.

Despite the significant work that has been done on cloning[1] and emulating[2] the 808 bass drum, there is an almost complete lack of published analyses on the circuit.[3] The history of the 808 is steeped in anecdote, and misinformation about its voice design still abounds. Although the fabric of lore surrounding the design, inception, and use of the 808 lends a richness to its overall mythology, they also give credence to a blithe sort of analog fetishism. The device's ingenious and satisfying properties are often attributed to mere circuit element nonlinearities. In addition to being inaccurate, this mindset directs attention away from a more interesting story. The designers of the 808's voice circuits[4] masterfully blended ingenuity and efficiency, creating circuits with great detail and complexity, but a part count low enough to be amenable to mass manufacture.[5]

The 808 was released just before the development of the MIDI standard (it used Roland's DIN sync protocol). As MIDI gained traction, users and technicians became accustomed to retrofitting the 808 with MIDI capabilities, also making extensive modifications to its voice circuitry.[6] This tradition parallels the development of circuit-bending and other music hardware hacking, and could unfortunately be lost in the process of digitally emulating an 808.[7]

The goals of this research are to partition the 808's bass drum circuit into functional blocks, create a physically-informed analysis of each block, model each block in software, and evaluate the results, paying special attention throughout to analysis of the circuit's behavior in terms of the electrical values of circuit elements (resistors and capacitors). These methods are well-represented in virtual analog literature,[8] but have not previously been used in the analysis of analog drum machine circuits.[9]

---

[1]Full analog clones such as the AcidLab Miami, clones of individual voices in a modular synth like the Analogue Solutions line of Concussor modules, and new drum machines using simplified 808 circuitry [3] are common (references are representative but far from comprehensive).

[2]The first 808 emulation, Propellerhead's sample-based ReBirth RB-338 [4], was introduced in 1997. Since then, there have been many commercial emulations based on structured sampling and black-box models. Marketing materials for the D16 Group's Nepheton mention circuit modeling. Roland's TR-8 Rhythm Performer, from their upcoming AIRA line, will employ their proprietary Analog Circuit Behavior (ACB) technique, presumably a form of physical modeling.

[3] [5] discusses [1] in the context of designing and building a hardware clone of the bass drum. [6] offers a qualitative description in the context of imitating classic bass drum sounds with other synthesizers. [7], which takes a control systems approach to designing an 808-inspired bass drum synthesizer, is a rare academic treatment.

[4]Roland president Ikutaro Kakehashi names Mr. Nakamura, though also indicates that it was a team effort [8].

[5]Robert Henke writes [9]: "The TR-808 is a piece of art. It's engineering art, it's so beautifully made. If you have an idea of what is going on in the inside, if you look at the circuit diagram, and you see how the unknown Roland engineer was making the best out of super limited technology, it's unbelievable. You look at the circuit diagram like you look at an orchestral score, you think, how on earth did they come up with this idea. It's brilliant, it's a masterpiece."

[6]for instance, Robin Whittle's professional modification work [10]

[7] [11] presents one approach to simulating circuit-bent instruments based solely on digital circuitry.

[8]For instance, [12] collects a representative set of references on modeling classic analog filters, and [13] is a comprehensive treatment of musical distortion circuits.

[9]However, [14] presents a physical and behavioral circuit model of the *digital* E-mu SP-12 sampling drum computer.
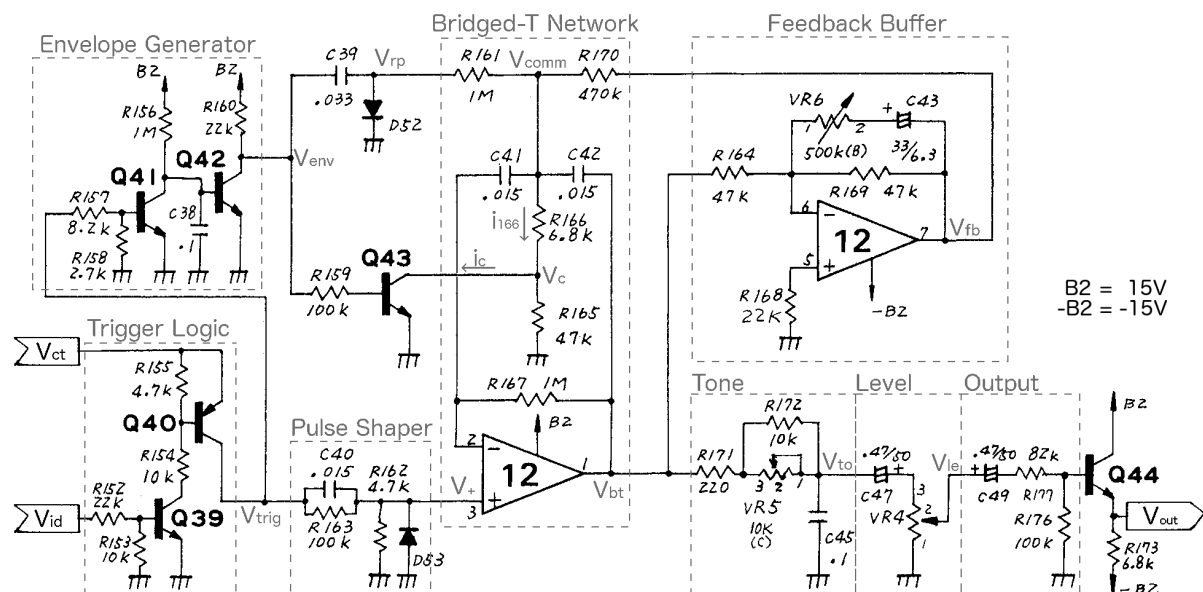
Figure 1: *TR-808 bass drum schematic, blocks marked (adapted from [1]).*

Our analysis of the circuit will clear up a host of common misconceptions about the 808 bass drum, including the role of device nonlinearities, the difference between the bass drum's characteristic pitch sigh and the frequency jump during the attack, and why unmodded bass drums can sound very different from one another.

Drawing on this analysis, we'll propose methods for software modeling of a modified/circuit-bent 808 bass drum circuit. By adopting a physically-informed approach, this work will avoid common pitfalls of software-based analog drum machine emulations, including the "machine gun effect," inaccurate behavior when a new note is triggered before the previous one has died out, and inaccurate behavior under various accent voltages.

In addition to the analysis itself, the primary result of this will be software that implements a circuit-bendable 808 bass drum.

An overview of the circuit is discussed in §2 and an analysis of each part of the the circuit and their interconnections is given in §§3–9. This is followed by a discussion of digital modeling techniques in §10 and results in §11.

2. OVERVIEW

Fig. 1 shows a schematic diagram of the TR-808 bass drum circuit. This schematic labels important nodes and currents, and emphasizes how the circuit can be broken down into blocks: trigger logic (see §3), a pulse shaper (see §4), a bridged-T network (see §5 and 7), a feedback buffer (see §6), an output tone and volume stage (see §9), and an envelope generator with complex behavior (see §8). Fig. 2 shows a block diagram of the digital model of the bass drum circuit. Both figures should be consulted alongside the analysis of each block in the following sections.

A bass drum note is produced when the μPD650C-085 CPU applies a common trigger and (logic high) instrument data to the trigger logic. The resulting 1-ms long pulse is delivered via the pulse shaper to the bridged-T network (a band pass filter), whose ringing produces the core of the bass drum sound. The 1-ms long pulse also activates an envelope generator, which alters the bridged-

T's center frequency for the first few milliseconds and supplies a retriggering pulse to the center of the bridged-T network after a few milliseconds. Leakage through the retriggering pulse circuit accounts for "sighing" of the bass drum's pitch.

Certain features of the bass drum sound are user-controllable. The output level is set by variable resistor (potentiometer) VR_4, the tone is set by VR_5, and the length of a bass drum note is controlled via VR_6.

Partitioning the circuit into blocks will serve the triple purpose of greatly simplifying the mathematics of the system, elucidating the design intent of each sub-circuit, and allowing for the design and simulation of "mods" and "bends" that affect the architecture of the bass drum (for instance: disconnecting the pitch sigh or bypassing the tone stage). These partitions are chosen so that they occur where high-input-impedance stages are driven by low-output-impedance stages, where loading effects between blocks are negligible [15].[10]

By favoring a clear analysis that elucidated the design intent, this work supports informed modifications/hacks/bends of the circuit. A more complicated analysis could obscure the logic of the device's construction, with minimal gains in accuracy. Framing the analysis in terms of component values simplifies the simulation of "mods" and "bends" based on component substitution (for instance: making the pitch tunable, extending the decay time, or changing the pitch envelope's timing).

Certain parts of the model assume small-signal conditions and linearity where they may not be strictly present. Op-amps (the bass drum uses a dual μPC4558 [16]) are assumed to be linear, feature zero output impedance, and have an infinite ability to source current. In reality, op-amps that are not designed for rail-to-rail performance (including the μPC4558) experience saturation as their output voltage approaches the power supply rails. Op-amps have a small (but non-zero) output impedance and feature internal protection circuitry to limit the amount of current they can source.

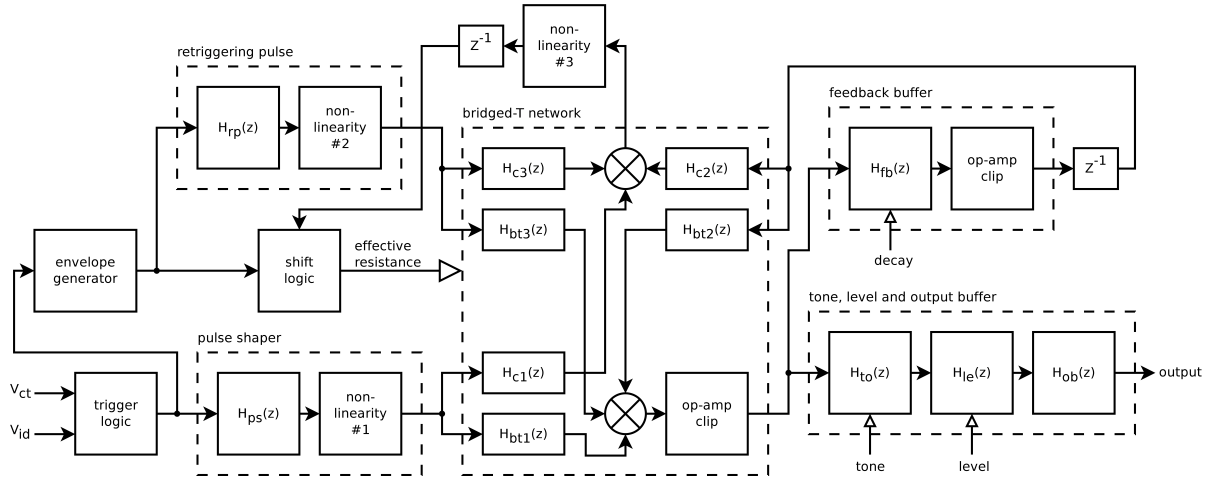[10]https://ccrma.stanford.edu/~jos/pasp04/Equivalent_Circuits.html

Figure 2: *TR-808 bass drum emulation block diagram.*

3. TRIGGER LOGIC

The CPU controls the timing and amplitude of each sound generator on the 808. A timing signal and accent signal are produced by the CPU, and combined into a common trigger signal (V_{ct}), whose ON voltage is set by a user-controllable global accent level. In general, instrument timing data (unique to each voice) sequenced by the CPU is "ANDed" with V_{ct} to activate individual sound generators.

In the case of the bass drum, the circuit comprised of Q_{39}–Q_{40} and R_{152}–R_{155} "ANDs" the instrument data (V_{id}) with V_{ct}. When V_{id} is present (logic high), a 1-ms long pulse with the same amplitude as V_{ct} (between 4–14 V, depending on VR₃) is passed to the collector of Q_{40}.

4. PULSE SHAPER

The pulse V_{trig} produced by the trigger logic drives a pulse shaper stage, which uses a nonlinear low shelf filter to deliver a shaped pulse to the bridged-T op-amp's inverting input (V_+). This circuit passes the high frequency components of input pulse, while "shaving off" the falling edge of the pulse. Fig. 3 shows the response of the pulse shaper to input pulses with a range of accents.

In the time domain, the output voltage swings immediately high in response to an applied trigger pulse, then smoothly settles down to $V_{TRIG}R_{162}/(R_{162}+R_{163})$. 1 ms later, when the applied pulse returns to ground, the output swings low and then starts to rise smoothly up to ground. It is important to note that the falling edge response is largely independent of the pulse amplitude - each time 0.71 V (approximately one diode drop) develops across D_{53}.

Since it is the edges of the shaped pulse that will kick the bridged-T network into oscillation, this analysis is concerned with the amplitude of each edge. The rising edge has an amplitude equal to the applied trigger voltage V_{TRIG}, and the falling edge has an amplitude approximately equal to $V_{TRIG}R_{162}/(R_{162}+R_{163}) + 0.71$.

4.1. Pulse Shaper ODE

An ordinary differential equation (ODE) describing the behavior of the pulse shaper will form a baseline for simulating it. First, re-
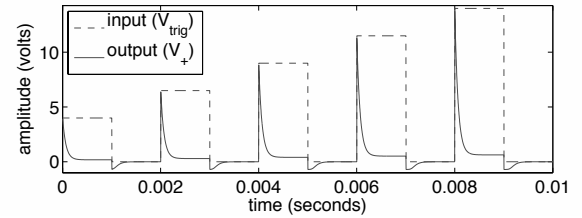

Figure 3: *Pulse shaper behavior under various input pulses.*

call the equations for the impedances of resistors and capacitors[11] and the Shockley ideal diode equation, which provides a model of the relationship between the current I and voltage V_D of a p–n junction diode:

$$I = I_s \left(e^{\frac{V_D}{V_T}} - 1 \right), \tag{1}$$

where I_S, the reverse bias saturation current ($\approx 10^{-12}$ A), and V_T, the thermal voltage (≈ 26 mV at room temperature), are properties of the device.

Nodal analysis yields an implicit nonlinear ODE of first order:

$$R_{162}R_{163}C_{40} \left(\frac{dV_{trig}}{dt} - \frac{dV_+}{dt} \right) - R_{162}V_{trig}$$
$$+ (R_{162} + R_{163}) V_+ - R_{162}R_{163}I_s \left(e^{\frac{-V_+}{nV_T}} - 1 \right) = 0. \tag{2}$$

Although it is possible to simulate ODEs like this with numerical methods,[12] good results can be obtained by cascading a linear filter into a memoryless nonlinearity [18]. This can be done by deriving a linear continuous-time transfer function by neglecting the diode, and developing a physically-informed, memoryless nonlinearity to account for the diode's clipping behavior for negative output voltages.

---

[11] $Z_R = R$ and $Z_C = \frac{1}{sC}$, where R is resistance, C is capacitance, and s is the differentiation operator on the complex plane (the "S plane").

[12] [17] provides a good discussion in the context of audio effect simulation.
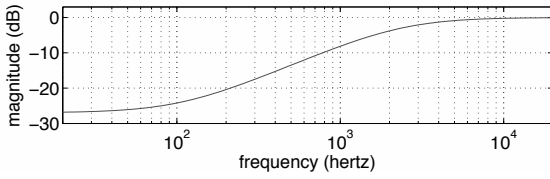
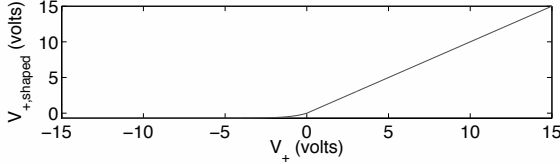Figure 4: *Pulse shaper shelf filter core, magnitude response.*

Figure 5: *Pulse shaper diode memoryless nonlinearity.*

An alternate approach to this method would be framing the pulse shaper as a time-variant filter after [19].

4.2. Shelf Filter Core

Neglecting the influence of the diode, the pulse shaper is a passive low shelf filter. Nodal analysis yields a continuous-time transfer function as a fraction of polynomials in s:

$$H_{ps}(s) = \frac{V_+(s)}{V_{trig}(s)} = \frac{\beta_1 s + \beta_0}{\alpha_1 s + \alpha_0}, \qquad (3)$$

with coefficients:

$$\begin{aligned}\beta_1 &= R_{162} R_{163} C_{40}\\ \beta_0 &= R_{162}\\ \alpha_1 &= R_{162} R_{163} C_{40}\\ \alpha_0 &= R_{162} + R_{163}.\end{aligned}$$

Evaluating this transfer function along the $s = j\omega$ axis and taking the magnitude yields the magnitude response of the filter core (shown in Fig. 4).

Note well that the DC response ($s = 0$) of this filter matches the observed response, $R_{162}/(R_{162}+R_{163})$.

4.3. Diode Memoryless Nonlinearity

A memoryless nonlinearity that approximates the diode's function, based on Eqn. (1) is:

$$V_{+,\text{shaped}} = \begin{cases} V_+ & \text{if} \quad V_+ \geq 0 \\ 0.71\left(e^{V_+} - 1\right) & \text{if} \quad V_+ < 0 \end{cases}. \qquad (4)$$

As shown in Fig. 5, it will not allow the output voltage to swing lower than approximately one diode drop, and leaves positive output voltages unaffected.

5. BRIDGED-T NETWORK

The bridged-T network is a Zobel network topology which found use in the measurement of high resistances at radio frequencies as

early as 1940 [20]. Bridged-T networks in this context were designed using the image-impedance principle to present the same impedance at both their input and output ports. In the 1970s, bridged-T networks found new use in analog drum machines.

When placed in the negative feedback path of an op-amp, a certain type of bridged-T network (capacitive "arms," and resistive "bridge" and path to ground) forms a band pass filter, which can be used to create decaying pseudo-sinusoids in response to impulsive input. This technique was known in the electronics hobbyist community as early as 1979[13] and used by drum machine manufacturers as early as 1976.[14] The 808 represented Roland's first implementation of the bridged-T network, and it was used in every single one of its sound generators in some form.[15]

The bass drum uses the most complicated form of the bridged-T network in the 808. It filters multiple inputs, including the output of the pulse shaper V_+, the output of the feedback buffer V_{fb}, and the retriggering pulse V_{rp} applied via R_{161}. The center frequency of the bridged-T network is subject to modulation (via Q_{43}) by the output of the envelope generator, as well as by leakage through R_{161}.

Ignoring the circuitry that will apply the retriggering pulse and the circuitry which modulates the bridged-T's center frequency, the transfer function $H(s) = V_{bt}(s)/V_+(s)$ is found by defining an intermediate node V_{comm}, and applying nodal analysis. Assuming ideal op-amp behavior, this yields a continuous-time transfer function:

$$H(s) = \frac{V_{bt}(s)}{V_+(s)} = \frac{\beta_2 s^2 + \beta_1 s + \beta_0}{\alpha_2 s^2 + \alpha_1 s + \alpha_0}, \qquad (5)$$

with coefficients:

$$\begin{aligned}\beta_2 &= R_{\text{effective}} R_{167} C_{41} C_{42}\\ \beta_1 &= R_{\text{effective}} C_{41} + R_{167} C_{41} + R_{\text{effective}} C_{42}\\ \beta_0 &= 1\\ \alpha_2 &= R_{\text{effective}} R_{167} C_{41} C_{42}\\ \alpha_1 &= R_{\text{effective}}(C_{41} + C_{42})\\ \alpha_0 &= 1.\end{aligned}$$

Evaluating along the $s = j\omega$ axis and taking the magnitude yields a magnitude response $H_{bt1}(s)$ for the simplified bridged-T core, shown in Fig. 6. Respecting superposition (grounding V_{rp} and V_{fb}), the substitution $R_{\text{effective}} = R_{161} \parallel (R_{165} + R_{166}) \parallel R_{170}$ can initially be used. Finding the proper value for $R_{\text{effective}}$ is non-trivial and will be a main focus of the rest of this analysis. Later, the output of the feedback buffer V_{fb} and the source of the retriggering pulse V_{rp} will be treated as second and third inputs to the bridged-T network, and modulations of $R_{\text{effective}}$ via Q_{43} will be considered.

This magnitude response shows a center frequency at ≈ 49.5 Hz,[16] which is close to the entry Roland's "typical and variable" tuning chart (56 Hz) [1] and the sound of a real 808 bass drum.

---

[13] see: "Rhythm Pattern Generator MM5871" [21, p. 48-49]

[14] It was used in the Korg's mini pops 120 bass drum and snare drum voices. The related twin-T circuit was used in the low and high congas [22].

[15] The TR-808 snare drum, lo/mid/hi tom/congas, and rim shot/clave all use bridged-T networks in similar ways to the bass drum, to create decaying pseudo-sinusoids in response to impulsive input. Bridged-T networks are also used as band pass filters in the remaining voices: handclap, cowbell, cymbal, and open/closed hihat.

[16] [1] provides an equation for the center frequency of a simple bridged-T network: $f_c = 1/\left(2\pi\sqrt{R_{\text{effective}}R_{167}C_{41}C_{42}}\right)$.
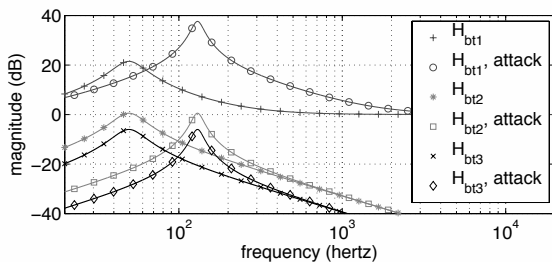
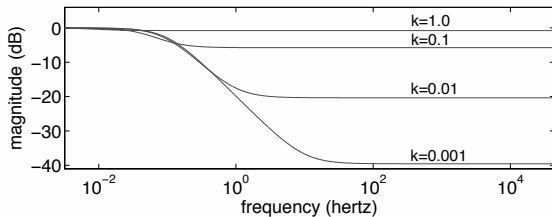Figure 6: *Magnitude responses of bridged-T network.*

Figure 7: *Family of feedback buffer magnitude responses, with various bass drum decay settings $k \in [0.001, 1.0]$.*

6. FEEDBACK BUFFER STAGE

The length of an 808 bass drum note is user-controllable via potentiometer VR_6, "bass drum decay," which affects the frequency response of the feedback buffer high shelf filter. The output of the bridged-T network is applied to the input of the feedback buffer stage, shaped by its frequency response, and then applied to R_{170}, another input to the bridged-T network. The less that the feedback buffer stage attenuates the signal passing through it, the longer the decay of the 808 note will be.

Assuming an ideal op-amp, there will be no current through, and therefore no voltage across, R_{168}. Nodal analysis yields a continuous-time transfer function:

$$H_{fb}(s) = \frac{V_{fb}(s)}{V_{bt}(s)} = \frac{\beta_1 s + \beta_0}{\alpha_1 s + \alpha_0}, \tag{6}$$

with coefficients:

$$\beta_1 = -R_{169} VR_6 k C_{43}$$
$$\beta_0 = -R_{169}$$
$$\alpha_1 = R_{164}(R_{169} + VR_6 k)C_{43}$$
$$\alpha_0 = R_{164},$$

where $VR_6 k$ is the resistance of the decay control with maximum resistance VR_6 and knob position $k \in [0.0, 1.0]$. The magnitude response for the feedback buffer is shown in Fig. 7.

7. BRIDGED-T IN FEEDBACK

When examining the bridged-T network in a feedback configuration, where its input is the output of the feedback buffer section, it will have a different transfer function. This topology is discussed in [23, p. 138].

Defining an intermediate node V_{comm} at the node joining R_{166}, C_{41}, and C_{42}, holding V_- at ground (apropos superposition theorem), applying ideal op-amp assumptions, and applying nodal analysis yields a continuous-time transfer function:

$$H_{bt2}(s) = \frac{V_{bt}(s)}{V_{fb}(s)} = \frac{\beta_1 s}{\alpha_2 s^2 + \alpha_1 s + \alpha_0}, \tag{7}$$

with coefficients:

$$\beta_1 = -R_\| R_{167} C_{41}$$
$$\alpha_2 = R_\| R_{167} C_{41} C_{42}$$
$$\alpha_1 = R_\| R_{170}(C_{41} + C_{42})$$
$$\alpha_0 = R_\| + R_{170}.$$

Again, superposition must be respected. $R_\|$ is the parallel combination $R_{161} \| (R_{165} + R_{166})$. The magnitude response $H_{bt2}(s)$ of the bridged-T in feedback is shown in Fig. 6.

8. FREQUENCY EFFECTS

Discussion of the 808's bass drum often conflates two phenomenon: a brief increase in the center frequency of the bridged-T network by more than an octave during the attack, and the 808's pitch sigh, a subtle modulation caused by leakage through R_{161}.

8.1. Frequency Shift on Attack

In addition to supplying a 1-ms wide pulse to the pulse shaper, the trigger logic also activates an envelope generator comprised of Q_{41}, Q_{42}, and surrounding resistors and capacitors. The output voltage V_{env} of this envelope generator (taken at the collector of Q_{42}) swings quickly up, and doesn't settle back down to ground until approximately 5 ms after the trigger swings low.

While the collector of Q_{42} is high, some current will flow into the base of Q_{43}. The effect of this is that the collector of Q_{43} gets grounded, and the $R_{effective}$ decreases from $R_{165} + R_{166}$ to R_{166}. So, the transfer functions describing the bridged-T networks behavior will change (labelled "attack"), raising both the Q and the center frequency, as shown in Fig. 6.

Although this brief change of center frequency (≈ 6 ms, less than a single period at the higher frequency) isn't long enough to be perceived as a pitch shift, it greatly affects the sound of the bass drum's attack, making it "punchier" and "crisper."

A few milliseconds after the start of a note, when the center frequency of the bridged-T network shifts down to its normal position, most of the energy at the normal center frequency will have been attenuated already. To keep the note from experiencing an abrupt jump in amplitude, the circuit composed of C_{39}, R_{161} and D_{52} applies a retriggering pulse to the bridged-T network.

A rough model of this can be obtained by treating the envelope applied at the collector of Q_{42} as an ideal voltage source V_{env} and treating V_{comm} as ground (as shown in Fig. 8). Now, the combination of C_{39}, R_{161} and D_{52} can be viewed as a simple high pass filter with a diode clipper across its output. This can be analyzed just like the pulse shaper from §4.

This retriggering pulse V_{rp} is applied to the bridged-T network through R_{161}. The transfer function $H_{bt3}(s) = V_{bt}(s)/V_{rp}(s)$ of this path through the bridged-T network is very similar to the feedback case discussed in §7, save an interchange of of R_{161} and R_{170}. Its magnitude response and the shifted version during the attack are shown in Fig. 6.
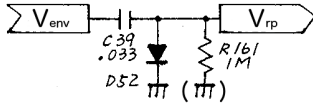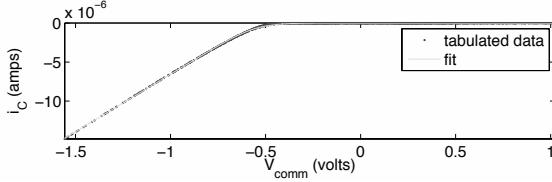
Figure 8: *Retriggering pulse filter.*

Figure 9: *Fit to memoryless nonlinearity relating V_{comm} and i_C.*

The length of the envelope and the timing of the retriggering pulse can be changed somewhat by changing C_{38}. Changes on R_{156} also affect biasing, and will have more complicated consequences.

8.2. Leakage and Pitch Sigh

Although the center frequency shift during attack is explained in §8.1, this effect is only active for the first few milliseconds of a note. It does not account for the bass drum's characteristic pitch sigh. This sigh is actually a consequence of leakage through R_{161}.

When V_{comm} swings low enough (below about one diode drop below ground), the base of Q_{43} gets lifted up and current flows into the base, causing even more current i_C to be drawn in through its collector. This current changes the effective resistance ($R_{\text{effective}}$, the ratio between V_{comm} and i_{166}, the current drawn through R_{166}), hence altering its transfer function and center frequency.

Although the physics of this part of the circuit are difficult to deal with in closed form, a few observations can lead to a simplified model with good properties. Using SPICE to simulate a stock bass drum note and tabulate V_{comm} and i_C, it is clear that their relationship is reasonably well-approximated by a memoryless nonlinearity, shown in Fig. 9.

This memoryless nonlinearity can be reasonably approximated using a parameterized equation sharing some topological similarity to Eqn. (1):[17]

$$i_C = -\log\left(1 + e^{-\alpha(V_{\text{comm}} - V_0)}\right)\frac{m}{\alpha}, \qquad (8)$$

where m is the slope of the response in the linear region, V_0 is the voltage offset of the "knee," and α is a parameter that controls the width of the transition region. These parameters are chosen by a three step fitting procedure. First, the method of least squares is used to estimate m and V_0 in the linear region only. These values of m and V_0 are tested with a line search over reasonable α values, again minimizing squared errors. Finally, a fine-grained brute-force search over a small neighborhood surrounding this fit yields some small improvements, and the fit parameters:

$$\alpha = 14.3150$$
$$V_0 = -0.5560$$
$$m = 1.4765 \cdot 10^{-5}.$$

---

[17]This is related to the physics of the p–n junction in Q_{43}, not D_{52}.

To get $R_{\text{effective}}$ in terms of just V_{comm}, i_c's effect on $R_{\text{effective}}$ must be taken into account. Considering the entire $R_{\text{effective}}$ branch of the bridged-T network (including i_C), defining an intermediate note V_C at the collector of Q_{43}, applying KCL, and rearranging yields:

$$R_{\text{effective}} = \frac{V_{\text{comm}}R_{166}\left(R_{165} + R_{166}\right)}{V_{\text{comm}}\left(R_{165} + R_{166}\right) - R_{165}\left(V_{\text{comm}} - R_{166}i_C\right)}. \qquad (9)$$

Note that, when $i_C = 0$, this reduces down to the trivial $R_{165} + R_{166}$, and that as i_C increases, $R_{\text{effective}}$ goes down. A low enough V_{comm} leads to a higher center frequency.

To apply this insight to the previously-derived transfer functions, the series combination of $R_{165} + R_{166}$ should be replaced by $R_{\text{effective}}$.

Furthermore, to change $R_{\text{effective}}$ in terms of V_{comm}, the model must keep track of V_{comm} as the sum of each of the bridged-T's inputs, using transfer functions H_{c1}, H_{c2}, and H_{c3}. The particulars of these transfer functions are related to their counterparts H_{bt1}, H_{bt2}, and H_{bt3}, and can be derived via nodal analysis.

9. TONE, LEVEL, AND OUTPUT BUFFERING STAGE

The bass drum's tone and level controls, and output buffering stage are simply a passive low pass filter, cascaded into a voltage divider, cascaded into a high pass filter.

There are non-negligible loading effects, but they mostly change the position of very low (sub-audible) poles. Since these discrepancies are minimal, inaudible, and are not part of a feedback configuration or upstream of a nonlinearity (where they might have more far-reaching effects), this work breaks this stage into three blocks and makes clear the function of each, despite nonzero connection currents and loading.

Nodal analysis yields first-order continuous-time transfer functions (summarized in Table 1) for each stage of the form:

$$H(s) = \frac{\beta_1 s + \beta_0}{\alpha_1 s + \alpha_0}. \qquad (10)$$

Table 1: Output Stage Continuous-Time Filter Coefficients.

Stage	β_1	β_0	α_1	α_0
Low pass	0	1	$R_{eq}C_{45}$	1
Level	$\text{VR}_6(1-m)C_{47}$	0	$\text{VR}_6 C_{47}$	1
High pass	$R_{177}C_{49}$	0	$R_{176}C_{49}$	1

In Table 1, R_{eq} is the equivalent resistance of the network formed by $R_{171} + (R_{172} \parallel \text{VR}_5)$:

$$R_{eq} = R_{171} + \frac{R_{172}\text{VR}_5 l}{R_{172} + \text{VR}_5 l}. \qquad (11)$$

$\text{VR}_5 l$ and $\text{VR}_6 m$ are the resistances of the tone and level controls with maximum resistances VR_5 and VR_6 and knob positions $l, m \in [0.0, 1.0]$.

10. MODELING

A digital model is implemented in Cycling 74's `Gen~`, a low-level DSP environment in `Max/MSP`. This model contains stock

controls for bass drum decay, tone, and level, as well as "bends" controlling tuning, attack tuning, extended decay, and input pulse width.

Memoryless nonlinearities are implemented directly, and the trigger logic can be implemented with simple algebraic manipulations on the accent level and timing data. All discrete-time filter coefficients are calculated with the bilinear transform. Although the bilinear transform has many nice properties (including order preservation, stability preservation, and avoiding aliasing), the fact that it maps from continuous-time frequency $\omega_a \in [-\infty, \infty]$ to discrete-time frequency $\omega_d \in (-\pi, \pi]$ means that it necessarily causes some frequency warping [15].[18] The bilinear transform constant c can be tuned to map one continuous-time frequency to precisely the right discrete-time frequency. This is not incorporated in this model, however, since salient filter features are at low frequencies with respect to the sampling rate. So, the standard untuned value of $c = {}^2/_T$ is used throughout [15].[19]

The choice of filter topology is particularly important, since many of the filter blocks (especially the bridged-T network) will feature time-varying coefficients. In the model, all filter blocks are implemented with Transposed Direct Form-II (TDF-II) topologies. The TDF-II topology has good numerical properties and behaves well under changing coefficient values, which is of special importance for the bridged-T network, with its constantly-shifting effective resistances. TDF-II seems sufficient, but in the future other filter topologies such as the normalized ladder filter [15][20] and Max Matthews' phasor filter [24] can be explored for even better properties under time-varying coefficients.

The feedback arrangement of the bridged-T network and the feedback buffer creates a delay-free loop. In the model, this can be addressed by inserting a unit delay after the feedback buffer, which will have only negligible effects on the frequency response.[21] Alternatively, the delay-free loop could be avoided by combining the analog prototypes in feedback before digitization via the bilinear transform.

Some parts of the analysis feature deviations from the behavior of the real device. In particular, the behavior of Q_{43} and the interaction between the bridged-T network and the envelope generator, though physically-informed, are oversimplified.

Where connection currents between sub-circuits would not be negligible, results could be improved by methods such as [25].

11. RESULTS

Fig. 10 shows a time-domain plot of the first 13 ms of a single bass drum note, showing good agreement between the physical model and a SPICE simulation.

Fig. 11 shows the estimated instantaneous frequency of the first 300 ms of a single bass drum note,[22] showing good agreement between the physical model and a SPICE simulation. Note well the unique characteristics of the pitch sigh.

---

[18] https://ccrma.stanford.edu/~jos/fp/Frequency_Warping.html

[19] https://ccrma.stanford.edu/~jos/pasp/Bilinear_Transformation.html

[20] https://ccrma.stanford.edu/~jos/pasp/Conventional_Ladder_Filters.html

[21] since all of the frequency response features are very low in frequency with respect to the sampling rate

[22] estimated by taking the Hilbert transform of the time-domain signal to obtain an analytic version, then estimating the derivative of its phase
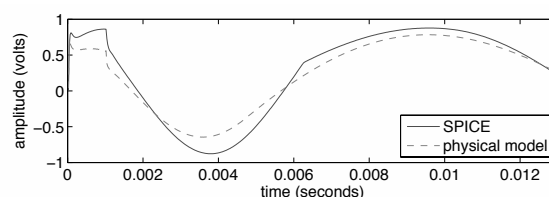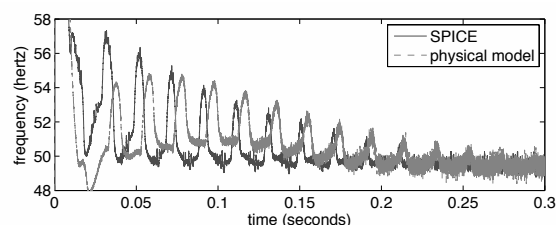

Figure 10: *Transient response.*

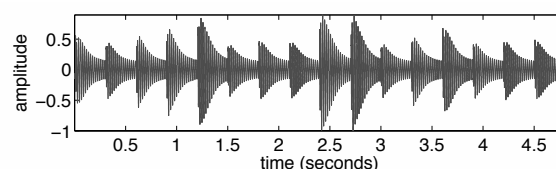Figure 11: *Estimated instantaneous frequency.*

Figure 12: *Lack of "machine gun effect" in model output.*

Fig. 12 shows a time-domain plot of the bass drum physical model when it is retriggered before the previous note has gone silent. Each note is slightly different, as in a real 808, since the remaining filter states may interfere constructively or destructively with the response to a new trigger—the model avoids the "machine gun effect."

In light of this analysis, variations in sound between individual 808s are easily understood as a consequence of the tolerances of the circuit elements (the voice circuits featured $\pm 20\%$ capacitors and $\pm 5\%$ resistors). These variations have significant effects on the gain, center frequency, Q, decay time, &c. of filter sections, especially when they are in feedback configurations (the bridged-T network and feedback buffer).

Audio examples and other supplementary materials can be found online at this work's companion page.[23]

12. CONCLUSION

In addition to informing a real-time computer model of the TR-808 bass drum, these findings will have many secondary applications. Due to the original hardware's value (and the danger of working with mains-powered electronics), 808 modifications are often quite conservative, and it has been a rare subject for circuit benders. This work supports the design of further modifications and can inform the design of future drum machines.

This research forms a foundation for musicological inquiry into Roland's line of analog drum machines, which traces roots

---

[23] https://ccrma.stanford.edu/~kwerner/papers/dafx14.html

back to Ace Tone's 1964 R1 Rhythm Ace.

The modeling of additional 808 voices will open the door for experimentation with flexible signal routings and feedback between voices and sub-circuits.

We've partitioned the circuit into blocks, and made a detailed first-order model of each block. The performance of this model makes it clear that the architecture of the 808 bass drum and complex interactions between subcircuits are more important than subtle device nonlinearities.

Even without tuning, a modeling scheme derived from this analysis shows the same features as a SPICE model and recordings of a TR-808 [26], including basic tuning and timing, a lack of the "machine gun effect" on quickly repeated notes, accurate transient behavior on different accent levels, and proper handling of the complicated Q and center frequency trajectories of the bridged-T network under the entire range of decay settings and accents. This correspondance is consistent with the results of informal listening tests.

13. ACKNOWLEDGMENTS

14. REFERENCES

[1] Roland Corporation, "TR-808 Service Notes, first edition," June 1981.

[2] Beastie Boys, "Hello Nasty," Compact Disc, July 1998.

[3] Micky Delp, "Anatomy of a Drum Machine," Available at http://mickeydelp.com/news/108-anatomy-of-a-drum-machine.html, July 31, 2012; accessed January 08, 2014.

[4] Propellorhead Software, "The Rebirth Museum," http://www.rebirthmuseum.com, September 2005.

[5] Eric Archer, "Blog archive » 808 clones," Available at http://ericarcher.net/devices/tr808-clone/, accessed January 08, 2014.

[6] Gordon Reid, "Synth Secrets: Practical Bass Drum Synthesis," *Sound on Sound*, July 2002; accessed January 8, 2014, Available at http://www.soundonsound.com/sos/Feb02/articles/synthsecrets0202.asp.

[7] John Pillans and James Ridgway, "ENGR3227 Analogue Electronics, Electronics Project: Bass Drum Synthesiser," Tech. Rep., Australian National University, 2006; accessed January 08, 2014, Available at http://users.cecs.anu.edu.au/~Salman.Durrani/_teaching/TB1.pdf.

[8] Mark Vail, *Vintage Synthesizers: Pioneering Designers, Groundbreaking Instruments, Collecting Tips, Mutants of Technology*, Backbeat Books, second edition, 2000.

[9] Derek Walmsley, "Monolake in full," *The Wire*, January 2010; accessed February 3, 2014, Available at http://thewire.co.uk/in-writing/interviews/monolake-in-full.

[10] Robin Whittle, "Modifications for the Roland TR-808," Available at http://www.firstpr.com.au/rwi/tr-808/, October 7, 2012; accessed January 08, 2014.

[11] Kurt James Werner and Mayank Sanganeria, "Bit Bending: an Introduction," in *Proceedings of the International Conference on Digital Audio Effects (DAFx-16)*, Maynooth, Ireland, September 2–5, 2013.

[12] Julian Parker and Stephano D'Angelo, "A Digital Model of the Buchla Lowpass Gate," in *Proceedings of the International Conference on Digital Audio Effects (DAFx-16)*, Maynooth, Ireland, September 2–5, 2013.

[13] David T. Yeh, *Digital Implementation of Musical Distortion Circuits by Analysis and Simulation*, Ph.D. thesis, Stanford University, 2009.

[14] David T. Yeh, John Nolting, and Julius O. Smith, "Physical and Behavioral Circuit Modeling of the SP-12 Sampler," in *Proceedings of the 33rd International Computer Music Conference (ICMC)*, Copenhagen, Denmark, August 30, 2007.

[15] Julius O. Smith, *Physical Audio Signal Processing*, http://ccrma.stanford.edu/~jos/pasp/, 2010; accessed January 2, 2104, online book.

[16] NEC Corporation, "μPC4558 data sheet," March 1993.

[17] David T. Yeh, Jonathan S. Abel, and Julius O. Smith, "Simulation of the Diode Limiter in Guitar Distortion Circuits by Numerical Solution of Ordinary Differential Equations," in *Proceedings of the International Conference on Digital Audio Effects (DAFx-10)*, Bordeaux, France, September 10–15, 2007.

[18] David T. Yeh, Jonathan S. Abel, and Julius O. Smith, "Simplified, physically-informed models of distortion and overdrive guitar effect pedals," in *Proceedings of the International Conference on Digital Audio Effects (DAFx-10)*, Bordeaux, France, September 10–15, 2007.

[19] Jaromir Macak and Jiri Schimmel, "Nonlinear Circuit Simulation Using Time-Variant Filter," in *Proceedings of the International Conference on Digital Audio Effects (DAFx-12)*, York, UK, September 17–21, 2009.

[20] P. M. Honnel, "Bridged-T Measurement of High Resistances at Radio Frequencies," *Proceedings of the Institute of Radio Engineers*, vol. 28, no. 2, pp. 88–90, February 1940.

[21] Forrest M. Mims III, *Engineer's Notebook: A Handbook of Integrated Circuit Applications*, Radio Shack, first edition, 1979.

[22] Keio Electronic Laboratory Corporation, "Korg mini pops 120 Service Manual," 1976.

[23] T. Deliyannis, Yichuang Sun, and J.K. Fidler, *Continuous-Time Active Filter Design*, CRC Press, first edition, 1999.

[24] Dana Massie, "Coefficient Interpolation for the Max Mathews Phasor Filter," in *Proceedings of the 133rd Audio Engineering Society convention*, San Francisco, CA, October 26–29, 2012.

[25] Jaromir Macak, "Guitar Preamp Simulation Using Connection Currents," in *Proceedings of the International Conference on Digital Audio Effects (DAFx-16)*, Maynooth, Ireland, September 2–5, 2013.

[26] Michael Fischer, "Roland TR-808 Rhythm Composer Sound Sample Set 1.0.0," September 1994.